Electronic structure and magnetism of $Sr_3Ru_2O_7$

D. J. Singh and I. I. Mazin
Center for Computational Materials Science, Naval Research Laboratory, Washington, DC 20375
(Received 11 August 2000; revised manuscript received 11 October 2000; published 27 March 2001)

The electronic structure of layered $Sr_3Ru_2O_7$ in its orthorhombic structure is investigated using density functional calculations. The band structure near the Fermi energy, consists of Ru t_{2g} states hybridized with O p orbitals. The yz and xz bands, which are largely responsible for the nesting related antiferromagnetic spin fluctuations in Sr_2RuO_4 split pairwise into even and odd combinations due to the interlayer coupling reducing the strength of the nesting. The xy bands show much less interplanar coupling as expected, and also less c-axis dispersion, so that the barrel-like sections are largely intact compared to the single layer material. The zone folding due to orthorhombicity yields small cylindrical lens shaped Fermi surfaces centered at the midpoints of the former tetragonal Γ-X lines. Fixed spin moment calculations indicate that tetragonal $Sr_3Ru_2O_7$ is borderline ferromagnetic but that orthorhombicity favors magnetism via a substantial magnetoelastic coupling. These results are related to experimental observations particularly in regard to magnetic properties.

DOI: 10.1103/PhysRevB.63.165101 PACS number(s): 75.10.Lp, 71.18.+y, 74.20.Mn

I. INTRODUCTION

Perovskite derived ruthenates $(Sr,Ca)_{n+1}Ru_nO_{3n+1}$ with nominally Ru^{4+} in an octahedral O environment display an extraordinarily varied set of physical properties. In the Sr series, the end members, $SrRuO_3$ and Sr_2RuO_4 are, respectively, an itinerant ferromagnet[1–5] and an unconventional superconductor, widely thought to have triplet pairing symmetry,[6,7] possibly of magnetic origin.[8–11] The Fermi surface and momentum-dependent spin fluctuations play key roles in the pairing in such scenarios for superconductivity. The corresponding Ca end points $CaRuO_3$ and Ca_2RuO_4, which differ structurally from the corresponding Sr compounds only by moderate lattice distortions, are a highly renormalized paramagnetic metal and an antiferromagnetic Mott insulator, respectively.[12–18] The multilayer Ruddlesden-Popper compounds in the series show a wide variety of magnetic orderings, metal insulator transitions, and unusual transport properties, with sample dependence.[14,20–25] Not surprisingly, strong magnetoelastic effects are found and have been emphasized both theoretically[5] and experimentally.[13,18,19]

Density functional calculations of the band structure and Fermi surfaces of superconducting Sr_2RuO_4 have been reported[26,27] and subsequently confirmed in detail by quantum oscillation experiments.[28–30] Angle resolved photoemission spectroscopy (ARPES) experiments[31,32] showed features very similar to those in the band calculations and quantum oscillation measurements but with small shifts. However, because of van Hove singularities near the Fermi energy, these shifts drastically affect the topology. The Fermi surfaces predicted by band calculations arise from three bands, one each from the three Ru t_{2g} orbitals hybridized with the in-plane and, to a lesser extent, apical O p states.[33,34] The Fermi surface structure, which is highly two dimensional, thus consists to zeroth order of planar sections perpendicular to k_x and k_y, coming from the yz and xz orbitals, and a round cylinder centered at Γ, derived from the xy orbital. These hybridize and reconnect to form three sections, a circular cylinder around Γ and square cylinders around Γ and X. Strong nesting features remain from the xz and yz derived sheets, which lead to soft spin-fluctuations around $\mathbf{k}=(2\pi/3a,2\pi/3a)$, as observed in neutron scattering.[35] We have pointed out earlier[9] that the interplay of these antiferromagnetic spin fluctuations and a broad Stoner background, related to the proximity to ferromagnetism, may lead to competing order parameter symmetries. However, the situation may be complicated by magnetoelastic effects, that is, mixing between spin and charge degrees of freedom, i.e., spin fluctuations and phonons, which could modify the pairing interaction, perhaps favoring triplet symmetries though the physics of this is not well understood.

Perhaps the most similar compound to Sr_2RuO_4 is the bilayer compound $Sr_3Ru_2O_7$.[36,37] It is closely related in structure, highly two-dimensional and metallic. Cao and co-workers reported ferromagnetism at 104 K with additional lower temperature transitions,[21] while other samples were not ferromagnetic at these temperatures but exhibited transitions below 20 K.[24,25] Meanwhile, Huang and co-workers found no evidence for any long range magnetic order down to 1.6 K (Ref. 42) and Perry, and Ikeda and co-workers report that single crystals grown by a floating zone technique are paramagnetic, with strongly enhanced susceptibility and high Wilson ratio, leading to the conclusion that the material is on the verge of ferromagnetism.[38–40] Initially, $Sr_3Ru_2O_7$ was reported to be tetragonal, $I4/mmm$, similar to Sr_2RuO_4.[36] However, subsequent measurements revealed at least disordered rotations of the octahedra.[41–43] Recently, Shaked and co-workers[43] have shown that the distortions are ordered and refined the crystal structure into space group $Bbcb$ with a rotation of approximately 7°. In contrast, superconducting Sr_2RuO_4 is stable in the tetragonal $I4/mmm$ structure, but has a rotational phonon mode that softens steeply from the Γ point to the zone boundary interacting with and crossing the acoustic branch [$\Sigma_3 E_u$, corresponding at (π,π) to the main instability that produces the orthorhombic structure in $Sr_3Ru_2O_7$].[45]

The electronic structure of $Sr_3Ru_2O_7$ has been studied using ARPES (Ref. 20) and density functional calculations[46] and reasonable agreement was obtained, although not all the predicted sheets were resolved experimentally. However,

 ©2001 The American Physical Society

Perry and co-workers recently reported low temperature Hall measurements on high quality ($\rho_{res} \approx 2\ \mu\Omega$ cm) single crystals that seem inconsistent with the calculated tetragonal Fermi surfaces.[39] The purpose of the present paper is to report density functional calculations of the electronic structure, fermiology, and magnetic properties using the orthorhombic *Bbcb* crystal structure.

II. STRUCTURE AND METHOD

The calculations were done using the general potential linearized augmented plane wave (LAPW) method including local orbital extensions to treat the upper core levels and relax linearization errors.[47,48] The calculations were done within the local density approximation using the Hedin-Lundqvist exchange correlation function. Spin polarized calculations used the same functional and the von Barth–Hedin spin scaling. Well converged basis sets and Brillouin zone samplings were used, similar to those described previously.[8,9,49] Calculations for the ideal tetragonal structure were based on the experimental structure of Ref. 36 which differs slightly from that used by Hase and Nishihara.[46] However, the calculated electronic structure is similar to that obtained by them. The calculations for orthorhombic $Sr_3Ru_2O_7$ are based on the neutron data of Shaked and coworkers obtained on samples that, similar to floating-zone grown single crystals, show a susceptibility peak around 20 K presumably due to magnetism (but see below).[43] We find that the Fermi surface near the center of the basal plane zone is quite sensitive to the Fermi energy, especially for small sheets, as discussed below. As such, care was taken to obtain the Fermiology for the orthorhombic case. In particular, we tested various samplings for the Fermi surfaces and velocities and found that a high sampling of 850 *k* points calculated by the LAPW method in the irreducible wedge of the zone was needed. To obtain the plotted Fermi surfaces we used two methods. The first was a symmetrized Fourier method interpolation on these 850 *k* points,[50] and the second a minimum contour curvature method, but no significant differences were found.[51] The presented plots for the orthorhombic case were made with the latter.

III. BAND STRUCTURE AND FERMIOLOGY

The calculated band structure and Fermi surfaces of tetragonal $I4/mmm$ $Sr_3Ru_2O_7$ are shown in Figs. 1 and 2, respectively. As may be seen, they are very similar to those reported previously by Hase and Nishihara.[46] As mentioned, the three Fermi surfaces of Sr_2RuO_4, which has one RuO_2 layer per cell, may be regarded as arising from the three Ru t_{2g} orbitals. The d_{xy} orbital gives rise to a round cylindrical electronlike sheet centered at Γ (Z) and the d_{xz} and d_{yz} orbitals provide flat sheetlike sections perpendicular to k_y and k_z, respectively, that after reconnection become square cylindrical sections around X and Γ along with strong nesting. To a first approximation, the Fermi surfaces of tetragonal $Sr_3Ru_2O_7$ may be thought of as deriving from the six same bands (three from each RuO_2 layer) with bonding-antibonding (odd-even) splittings[44] due to the interaction between the RuO_2 sheets comprising the bilayer. However, as may be seen from the lack of fourfold symmetry around the X point in Fig. 2, there is more k_z dispersion in tetragonal $Sr_3Ru_2O_7$ than in Sr_2RuO_4, particularly for the even bands.

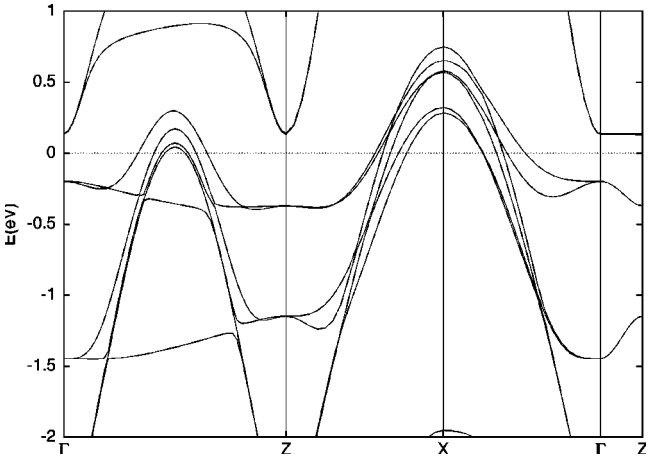

FIG. 1. Band structure of $Sr_3Ru_2O_7$ in the ideal tetragonal structure near the Fermi energy.

There is an approximately square cylindrical hole pocket around X, deriving from the odd combinations of d_{xz} and d_{yz} orbitals. Another cross-shaped hole pocket arises from reconnected sections of the Fermi surfaces of the even and odd parity with the same orbital character. The even combination also provides the innermost cylinder around Γ, which similar to the other three Γ centered cylinders is electronlike. The second Γ centered electronlike cylinder is also mainly d_{xz}/d_{yz} derived near the (10) directions, but is mixed with the d_{xy} character near (11). The two remaining Γ/Z centered cylinders are derived from the d_{xy} orbitals, and have very little even-odd splitting, in accord with their strongly in-plane orbital character. The three outer Γ centered cylinders change topology as the electron count is increased as they touch along the basal plane Γ-Z lines giving rise to the van Hove singularities seen above E_F in the density of states, as in Sr_2RuO_4. It is noteworthy that even before considering the effects of orthorhombicity, the Fermi surface nesting is con-

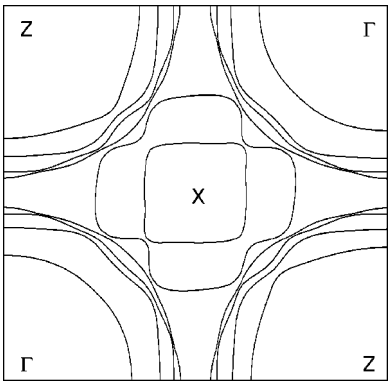

FIG. 2. Basal plane Fermi surface of $Sr_3Ru_2O_7$ in the ideal tetragonal structure. Note that because of interpolation in the plotting program (even-odd) crossings that occur in this plane become very small anticrossings.

siderably reduced relative to Sr_2RuO_4. This is due to (i) the even-odd splittings, (ii) the k_z dispersions, and (iii) the strong anticrossings of the even d_{xz}/d_{yz} and the odd d_{xy} bands. The striking difference from Sr_2RuO_4 stems from the fact that nearest neighbor hopping between d_{xz}/d_{yz} and d_{xy} orbitals is forbidden within a single layer, but allowed across the layers in a bilayer. A $d_{xz}(d_{yz})$ orbital hybridizes with the d_{xy} of the opposite parity, and this is the strongest at $k=\{0,\pi/a\}$ $(\{\pi/a,0\})$. Correspondingly, the strongest distortion of the xz/yz band occurs near the (1,1) directions. Note that additional hybridization between the xz/yz band and the xy band (and the only one existing in Sr_2RuO_4) happens due to hopping across the SrO layer. Depending on k_z, this hopping is of the same $(k_z=0)$ or of the opposite sign with respect to the intrabilayer hopping. This brings about an additional k_z dispersion.

Given the reduced nesting in $Sr_3Ru_2O_7$, one may conjecture that the incommensurate antiferromagnetic spin fluctuations seen in neutron scattering experiments[35] on Sr_2RuO_4 may be considerably less prominent in $Sr_3Ru_2O_7$. On the other hand, tetragonal $Sr_3Ru_2O_7$ is much closer to a ferromagnetic instability. This is not surprising considering the high value of the calculated density of states (DOS) at the Fermi energy (E_F), $N(E_F)=4.5$ states/eV Ru, compared with 4.1 states/eV Ru for Sr_2RuO_4.[27]

Nonspin-polarized local spin density approximation (LSDA) calculations for the orthorhombic structure yield a still slightly larger $N(E_F)=5.0$ states/eV Ru and the structure of the density of states around E_F is different (with larger magnitudes corresponding to slightly narrower t_{2g} bands, as shown in Fig. 3). The result is a magnetic ground state. However, before turning to the magnetic properties, we discuss the electronic properties of the nonspin-polarized system. As the magnetism has substantially itinerant character (see below) the nonspin-polarized electronic structure is expected to be a reasonable approximation for the paramagnetic phase well above any ordering temperature.

As a reference point, we show in Fig. 4 the Fermi surfaces of the tetragonal structure, but folded into the $Bbcb$ orthorhombic zone. This zone is half the area of the tetragonal zone due to the cell doubling and is rotated by 45°. The most striking feature of the folding is the development of cylindrical lens shaped Fermi surfaces centered at the midpoints of the Γ-Z lines (the midpoints of the Γ-X and Z-X lines in the tetragonal zone). These come from the two d_{xy} circular cylinders around Γ and the outer (odd) d_{xz}/d_{yz} cylinder.

One may expect that such folded Fermi surfaces and particularly the lenses should become observable in quantum oscillation experiments in samples with ordered orthorhombic structures, and possibly in photoemission as shadow Fermi surfaces with strength related to the matrix elements produced by the orthorhombic distortion even in samples where the distortion is not fully long-range ordered, as long as the in-plane coherence length is large enough (in analogy with some of the cuprate superconductors).[52–55] However, the actual distortion is a rotation of approximately 7°, which is not so small, and considerably changes the Fermi surfaces beyond the naive zone folding picture.

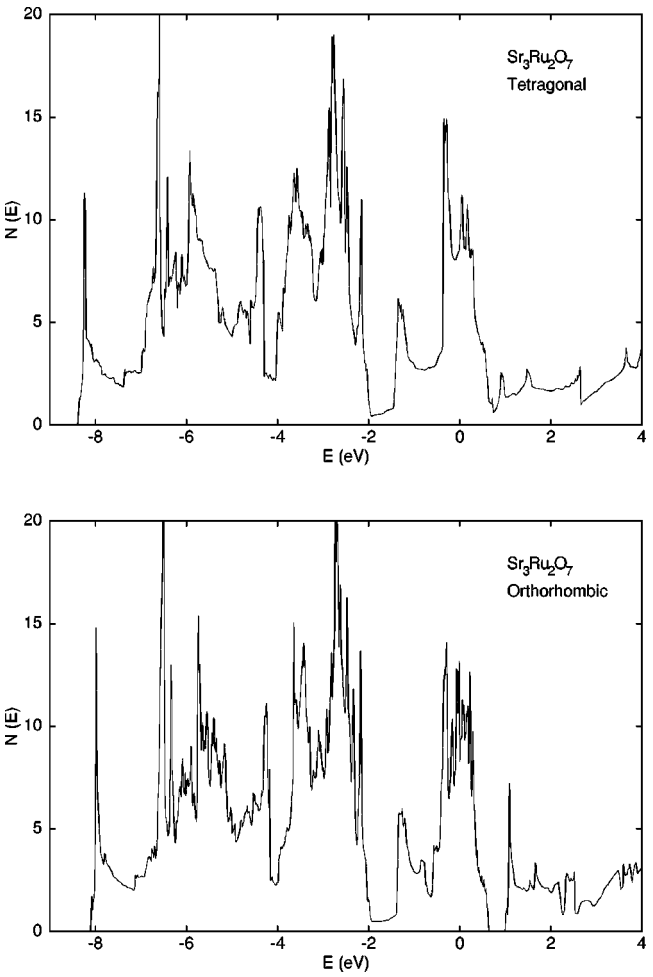

FIG. 3. Electronic density of states of ideal tetragonal (top) and orthorhombic (bottom) $Sr_3Ru_2O_7$ on a per formula unit basis. Energies are relative to E_F.

In fact, significant differences between the folded tetragonal and calculated orthorhombic Fermi surfaces are found, as shown in Fig. 5. Hybridization gaps open where folded bands cross. As a result, the square sections around the center of Fig. 4, which came from the overlap of the d_{xy} derived bands, entirely disappear, while the larger square section de-

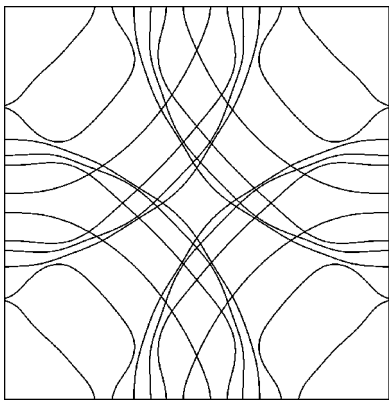

FIG. 4. Basal plane Fermi surface of $Sr_3Ru_2O_7$ in the ideal tetragonal structure folded into the orthorhombic zone (see text).

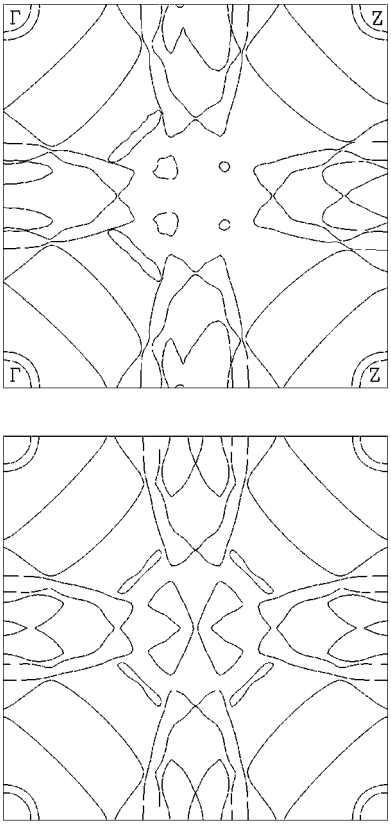

FIG. 5. Basal plane (top) and midplane (k_z shifted by 1/4, bottom) Fermi surfaces of $Sr_3Ru_2O_7$ in the experimental orthorhombic structure. Note that the zone is rotated 45° with respect to the tetragonal and folded.

rived from the odd d_{xz}/d_{yz} bands reconnects with the outer lens derived from the d_{xy} bands. One can see remnants of this square in the dents near the tips of the outer lenses in the orthorhombic structure. Also two small circular electron cylinders are introduced around the Γ-Z lines, with hardly any z dispersion; these are the bottoms of the $d_{x^2-y^2}$ bands, which in the tetragonal structure were located a few mRy above the Fermi level (Fig. 1). The lenses are now considerably distorted, because of the abovementioned interaction with the odd combination of d_{xz}/d_{yz} states, and because of the increased the k_z dispersion (note the lack of reflection symmetry about the center line in Fig. 5). Interestingly, this dispersion is concentrated mostly in small and/or heavy sections, so the average (r.m.s.) Fermi velocity remains quite two dimensional, i.e., $v_x \approx v_y = 1.3 \times 10^7$ cm/s and $v_z = 0.16 \times 10^7$ cm/s. Within the constant scattering time approximation this implies a resistivity anisotropy $\rho_c/\rho_a \approx 70$ as compared to the LDA value for Sr_2RuO_4 of ≈ 300, which is known to be an underestimate relative to experiment. Clearly, the bilayer compound is much more three dimensional than the single layer one, and this, presumably, moves it still further from an antiferromagnetic instability in-plane.

Finally, it should be mentioned that, because of the hybridization gaps near the center of the Brillouin zone of Fig. 5, the Fermi surface in this region is highly sensitive to the band filling. This is illustrated in Fig. 6, where Fermi surfaces calculated with 5 meV upwards and downwards shifts

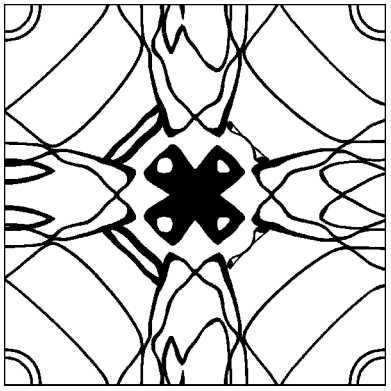

FIG. 6. Fermi surfaces of orthorhombic $Sr_3Ru_2O_7$ as in Fig. 5 but with filled areas indicating the effect of 5 meV upwards and downwards shifts of E_F.

of E_F are shown, so that the thickness of the lines is inversely proportional to the local Fermi velocity. This is also evident from the band structure, shown in Fig. 7, which features a complex of bands with avoided crossings near E_F around the zone center (center of the long Γ-Z line). Considering the fact that LDA calculations are sensitive to structural details and in any case should not be relied on at the 5 meV level, the topology in this region cannot be decided based on the present calculations. Because of this uncertainty, we cannot unambiguously match our results with the Hall measurements of Perry and co-workers,[39] but the possibility, suggested by them, that orthorhombicity provides a way of reconciling their measurements with band calculations seems plausible. If we restrict ourselves to the ''stable'' sheets of the Fermi surface, we observe two electronic $d_{x^2-y^2}$ derived cylinders, the hole pseudosquare and the hole pseudocross formed by the d_{xz}/d_{yz} bands, and several sets of lenses, all electronic. The complicated shape and changing curvature of these surfaces prevents us from associating the volumes of these Fermi surface pockets with Hall numbers. The only conclusion we can draw is that there is no clear way to guess the Hall conductivity from the electronic structure of the corresponding tetragonal compound. Furthermore, as seen from Fig. 6, shifting the chemical potential by as little as 5 meV (corresponding to 55 K) drastically changes the topology of the paramagnetic Fermi surfaces. The message of this observation is that substantial and nontrivial temperature dependencies of the Hall coefficient may occur independent of any anomalous Hall contribution.

IV. MAGNETISM

As mentioned, in the idealized tetragonal structure, $Sr_3Ru_2O_7$ is found to be paramagnetic in the LSDA, but with a very high susceptibility. In fixed spin moment calculations, moments up to $0.6\mu_B$/Ru are induced with an energy cost of less than 4 meV/Ru—a number almost indistinguishable from zero considering the accuracy of the present calculations. The orthorhombic distortion narrows the t_{2g} manifold and increases the density of states leading to a magnetic ground state via the Stoner mechanism. Furthermore, the paramagnetic orthorhombic band structure shows extremely

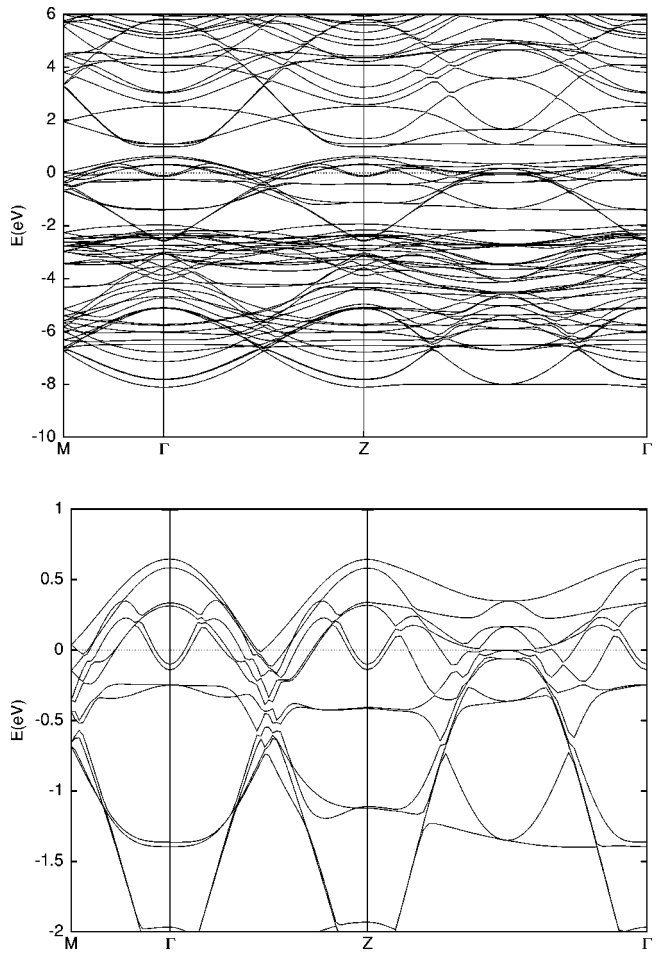

FIG. 7. Band structure of $Sr_3Ru_2O_7$ in the orthorhombic structure (top) and a blow-up near the Fermi energy (bottom). All the directions shown are in the basal plane. The shorter Γ-*Z* line is $[\alpha,0,\alpha/2.]$ (Γ-*Z* edge of the top Fermi surface plot, Fig. 5), while the longer Γ-*Z* line is $[\alpha,\alpha,\alpha/2]$ (a diagonal of the top Fermi surface plot), and *M* denotes the point [0,1/2,0] (midpoint of a Γ-Γ edge), all in reciprocal lattice coordinates.

flat bands near the *X* point (see Fig. 6), which create a low weight but extremely sharp peak within a few K from the Fermi level. Such a band structure is intrinsically unstable against any symmetry lowering splitting of this peak, including a magnetic instability. However, since the orthorhombic unit cell is already doubled, an antiferromagnetic instability would work just as well. There is nevertheless a strong reason for the system to prefer the ferromagnetic coupling in plane. Generally speaking, the electronic structure of Ru based perovskites shows strong Ru *d* O *p* hybridization and this favors ferromagnetic couplings[5] (O *p* states have rather large Hund rule coupling). Within a local picture, this tendency may be viewed as resulting from the fact that the density of states has substantial O weight around E_F and all things being equal, this favors magnetic configurations where the O can polarize, i.e., ferromagnetism. Within a simple Stoner picture, this O contribution to the magnetic energy is proportional to the square of the O contribution to the density of states around E_F. Decomposing $N(E_F)$ onto the LAPW spheres,[49] we find 56% Ru *d*, 20% plane O *p*, 2% apical (rocksalt) O *p*, and 3% bridging (interlayer) O *p*, with the remainder divided between other angular momentum characters (2%), and the interstitial (17%). Considering the ionic radii, the interstitial contribution is likely more O *p* than Ru *d* derived, but in any case, there is substantial O *p* involvement in $N(E_F)$ and this contribution is dominated by the in-plane oxygen. Not surprisingly then, ferromagnetic in-plane configurations are favored. We find a self-consistent ferromagnetic (FM) solution with a spin magnetization of 0.80 μ_B/Ru and an energy of -23 meV/Ru relative to the nonspin-polarized case. Calculations were also performed for antiferromagnetic configurations with a (2×2) in-plane ordering, and having adjacent Ru ions in the two planes of the bilayer polarized parallel. However, no self-consistent magnetic configuration was found. Thus it may be concluded that the magnetic character *within each plane* is itinerant. However, calculations in which the Ru ions in a layer were ferromagnetically aligned, but the layers were stacked antiferromagnetically (so each bilayer had one spin up and one spin down RuO_2 layer) did yield a stable magnetic solution (denoted AF-*A* in the following), in this case with an energy of -20 meV/Ru and a Ru moment (as measured by the moment in a Ru sphere) only 14% smaller than the ferromagnetic solution.

The energy difference between the FM and AF-*A* solutions contains two parts, within the most simple model. The first is the interaction between the two planes comprising the bilayer. This, in turn, has a ferromagnetic part originating from the Hund rule energy on the bridging oxygen, and an antiferromagnetic superexchange. Based on the calculation, we conclude that the former is slightly stronger. In any case, it is likely larger than the interbilayer coupling through the rock-salt layers. This expectation is based on the geometry (hopping via two oxygens with unfavorable bond angles) and the fact that the k_z dispersion is considerably less than the antisymmetric, symmetric band splittings due to the interaction between the planes comprising the bilayer. (Note that the exchange constants are usually quadratic in hopping and the dispersion linear.) Further, we note that calculations for Sr_2RuO_4, which has similar rock-salt layers and, of course, the same Ru valence, show a very weak, 0.1 meV antiferromagnetic interlayer coupling.[56] Now we speculate about the consequences as they may relate to experiment in a likely scenario.

Supposing that the interbilayer interaction is antiferromagnetic (as expected for a superexchange coupling) and much weaker than the intrabilayer coupling, one may conclude that the latter is ferromagnetic with a strength of order 3 meV/Ru. In this scenario, the ground state is antiferromagnetic, consisting of ferromagnetic bilayers, stacked antiferromagnetically.

This represents a conceptually interesting case for the Kosterlitz-Thouless theory of quasi-2D magnetic phase transitions.[57] The difference from the textbook case is that the in-plane magnetism is itinerant; the same qualitative picture applies, still, and so the 3D long-range order (LRO) transition temperature should be logarithmically suppressed compared to the ferromagnetic-paramagnetic energy difference. We can safely assume that the interbilayer coupling is

less than 30 K (the interplane coupling within a bilayer), probably very much less, thus bringing about a substantial Kosterlitz-Thouless suppression. One would, however, expect strong itinerant spin fluctuations of ferromagnetic character in planes for temperatures well above the LRO transition temperature; these should manifest themselves, for instance, in specific heat and magnetic susceptibility.

Very recently, Ikeda and co-workers reported a detailed study of single crystal floating-zone $Sr_3Ru_2O_7$ including magnetic susceptibility, specific heat and resistivity plus magnetic measurements under pressure.[40] They report a susceptibility maximum at $T_{max}=16$ K accompanied by structure in the resistivity, but conclude that long range antiferromagnetic order does not set in, based on the high nearly isotropic $\chi(T)$ below T_{max} and thus that the ground state is a paramagnetic Fermi liquid on the verge of ferromagnetism. In fact, the measured $\chi(T)$ is ~ 15 times larger than that of Sr_2RuO_4 (Ref. 58) and at least as isotropic at low T. Certainly, this is not expected with simple local moment ordered magnetism, especially in a material with strong magnetocrystalline anisotropy as is the case for magnetic ruthenates.[3] However, things are less clear cut in the itinerant metallic scenario above. First of all, in the ordered itinerant case, there is a Stoner continuum that contributes to $\chi(T)$ along the direction of the moments [the low $\chi(T)$ direction]; normally this is a very small effect, but here the magnetocrystalline anisotropy is expected to be very large[3] and the Fermi liquid very soft as evidenced by the strong Stoner renormalizations. Secondly, it should be noted that as long as the anisotropy is not in the trivial *c*-axis direction, the twinning of orthorhombic samples will mean that there will be no orientation where the applied field is aligned with the moments, again presumably lowering the anisotropy of χ in the magnetic state. However, both of these mechanisms for lowering the anisotropy in χ would require fortuitous strong numerical coincidences to explain the observed isotropy of the measured χ in a magnetically ordered state. On the other hand, the measured temperature dependence of the two components of χ is notably different, which is not simply anticipated for a standard enhanced paramagnet either. Another interesting possibility is to associate the peak in $\chi(T)$ not with LRO antiferromagnetic ordering, but with a Kosterlitz-Thouless type transition associated with the 2D bilayers. In this case, there would be no long-range magnetic order below the peak, though the weak interbilayer interactions could still yield a 3D ordered magnetic state at very low temperatures. This scenario would also provide a convenient explanation of the so called magnetic metallic phase in the $Ca_{2-x}Sr_xRuO_4$ phase diagram between $x=0.2$ and $x=0.5$ where an unusual phase with a peak in $\chi(T)$ is entered just as the system reaches an incipient ferromagnetic instability with x decreasing through 0.5.[18]

Finally, under applied pressures of 1 GPa Ikeda and co-workers[40] report evidence for ferromagnetism though with small moments ($M\approx 0.08\mu_B$/Ru) starting at 70 K based on magnetization measurements. While low moment ferromagnetism with this Curie temperature cannot be excluded, such a high ratio of T_C/M is unusual in traditional materials. Weak ferromagnetism due to canting seems to be more likely and also fits better with our calculations. We note that the ordering temperature in such a scenario would be sensitive to the out-of-plane superexchange coupling, which in turn is expected to increase strongly under pressure.

V. SUMMARY AND CONCLUSIONS

Density functional studies of $Sr_3Ru_2O_7$ show a substantial coupling of the electronic and magnetic properties with the octahedral rotations associated with the orthorhombic distortion. In particular, the Fermi surface nesting (already lower than in Sr_2RuO_4) is further reduced and the t_{2g} manifold is narrowed leading to magnetic tendencies. Using the experimental crystal structure[43] we find that the 2D RuO_2 planes form an itinerant system with ferromagnetic ordering tendencies, and additionally that the coupling between the two such planes comprising a bilayer is weak, but also ferromagnetic. We argue that the *c*-axis coupling between bilayers is weaker still and based on speculate that the magnetic character should be highly two dimensional, perhaps exhibiting Kosterlitz-Thouless physics.

ACKNOWLEDGMENTS

We are grateful for helpful discussions with C.S. Hellberg, J.D. Jorgensen, J.W. Lynn, A.P. Mackenzie, S. Nakatsuji, and M. Sigrist. We thank J.D. Jorgensen for a preprint of Ref. 43. Computations were performed using facilities of the DoD HPCMO ASC center. Work at the Naval Research Laboratory was supported by the Office of the Naval Research.

[1] J.J. Randall and R. Ward, J. Am. Ceram. Soc. **81**, 2629 (1959).
[2] J.M. Longo, P.M. Raccah, and J.B. Goodenough, J. Appl. Phys. **39**, 1327 (1968).
[3] A. Kanbayashi, J. Phys. Soc. Jpn. **44**, 108 (1978).
[4] D.J. Singh, J. Appl. Phys. **79**, 4818 (1996).
[5] I.I. Mazin and D.J. Singh, Phys. Rev. B **56**, 2556 (1997).
[6] Y. Maeno, H. Hashimoto, K. Yoshida, S. Nishizaki, T. Fujita, J.G. Bednorz, and F. Lichtenberg, Nature (London) **372**, 532 (1994).
[7] T.M. Rice and M. Sigrist, J. Phys.: Condens. Matter **7**, L643 (1995).
[8] I.I. Mazin and D.J. Singh, Phys. Rev. Lett. **79**, 733 (1997).
[9] I.I. Mazin and D.J. Singh, Phys. Rev. Lett. **82**, 4324 (1999).
[10] Y. Kitaoka, K. Ishida, K. Asayama, S. Ikeda, S. Nishizaki, Y. Maeno, K. Yoshida, and T. Fujita, Physica C **282-287**, 210 (1997).
[11] H. Mukuda, K. Ishida, Y. Kitaoka, K. Asayama, Z. Mao, Y. Mori, and Y. Maeno, J. Phys. Soc. Jpn. **67**, 3945 (1998).
[12] S. Nakatsuji, S. Ikeda, and Y. Maeno, J. Phys. Soc. Jpn. **66**, 1868 (1997).

[13] M. Braden, G. Andre, S. Nakatsuji, and Y. Maeno, Phys. Rev. B **58**, 847 (1998).
[14] A.V. Puchkov, M.C. Schabel, D.N. Basov, T. Startseva, G. Cao, T. Timusk, and Z.-X. Shen, Phys. Rev. Lett. **81**, 2747 (1998).
[15] G. Cao, S. McCall, J. Bolivar, M. Shepard, F. Freibert, P. Henning, J. Crow, and T. Yuen, Phys. Rev. B **54**, 15 144 (1996).
[16] G. Cao, S. McCall, M. Shepard, J.E. Crow, and R.P. Guertin, Phys. Rev. B **56**, 321 (1997).
[17] G. Cao, S. McCall, M. Shepard, J.E. Crow, and R.P. Guertin, Phys. Rev. B **56**, 2916 (1997).
[18] S. Nakatsuji and Y. Maeno, Phys. Rev. Lett. **84**, 2666 (2000).
[19] R. Matzdorf, Z. Fang, Ismail, J. Zhang, T. Kimura, Y. Tokura, K. Terakura, and E.W. Plummer, Science **289**, 746 (2000).
[20] A.V. Puchkov, Z.-X. Shen, and G. Cao, Phys. Rev. B **58**, 6671 (1998).
[21] G. Cao, S. McCall, and J.E. Crow, Phys. Rev. B **55**, 672 (1997).
[22] G. Cao, S. McCall, J.E. Crow, and R.P. Guertin, Phys. Rev. Lett. **78**, 1751 (1997).
[23] G. Cao, S.C. McCall, J.E. Crow, and R.P. Guertin, Phys. Rev. B **56**, 5387 (1997).
[24] S. Ikeda, Y. Maeno, and T. Fujita, Phys. Rev. B **57**, 978 (1998).
[25] R.J. Cava, H.W. Zandbergen, J.J. Krajewski, W.F. Peck, Jr., B. Batlogg, S. Carter, R.M. Fleming, O. Zhou, and L.W. Rupp, Jr., J. Solid State Chem. **116**, 141 (1995).
[26] T. Oguchi, Phys. Rev. B **51**, 1385 (1995).
[27] D.J. Singh, Phys. Rev. B **52**, 1358 (1995).
[28] A.P. Mackenzie, N.E. Hussey, A.J. Driver, S.R. Julian, Y. Maeno, S. Nishizaki, and T. Fujita, Phys. Rev. B **54**, 7425 (1996).
[29] A.P. Mackenzie, S.R. Julian, G.G. Lonzarich, Y. Maeno, and T. Fujita, Phys. Rev. Lett. **78**, 2271 (1997).
[30] C. Bergemann, S.R. Julian, A.P. Mackenzie, S. Nishizaki, and Y. Maeno, Phys. Rev. Lett. **84**, 2662 (2000).
[31] T. Yokoya, A. Chainani, T. Takahashi, H. Katayama-Yoshida, M. Kasai, and Y. Tokura, Phys. Rev. Lett. **76**, 3009 (1996).
[32] D.H. Lu, M. Schmidt, T.R. Cummins, S. Schuppler, F. Lichtenberg, and J.G. Bednorz, Phys. Rev. Lett. **76**, 4845 (1996).
[33] C. Noce, and M. Cuoco, Phys. Rev. B **59**, 2659 (1999).
[34] I.I. Mazin, D.A. Papaconstantopoulos, and D.J. Singh, Phys. Rev. B **61**, 5223 (2000).
[35] Y. Sidis, M. Braden, P. Bourges, B. Hennion, W. Reichardt, Y. Maeno, and Y. Mori, Phys. Rev. Lett. **83**, 3320 (1999).
[36] H.K. Muller-Buschbaum, and J. Wilkens, Z. Anorg. Allg. Chem. **591**, 161 (1990).
[37] M. Itoh, M. Shikano, and T. Shimura, Phys. Rev. B **51**, 16 432 (1995).
[38] S.I. Ikeda and Y. Maeno, Physica B **259-261**, 947 (1999).
[39] R.S. Perry, L.M. Galvin, A.P. Mackenzie, D.M. Forsythe, S.R. Julian, S.I. Ikeda, and Y. Maeno, Physica B **284**, 1469 (2000).
[40] S.I. Ikeda, Y. Maeno, S. Nakatsuji, M. Kosaka, and Y. Uwatoko, cond-mat/0002147 v2 (unpublished).
[41] Y. Inoue, M. Hara, Y. Koyama, S. Ikeda, Y. Maeno, and T. Fujita, in *Advances in Superconductivity IX*, edited by S. Nakajima and M. Murakami (Springer-Verlag, Berlin, 1997), p. 281.
[42] Q. Huang, J.W. Lynn, R.W. Erwin, J. Jarupatrakorn, and R.J. Cava, Phys. Rev. B **58**, 8515 (1998).
[43] H. Shaked, J.D. Jorgensen, O. Chmaissem, S. Ikeda, and Y. Maeno, J. Solid State Chem. **154**, 361 (2000).
[44] This may seem counterintuitive; however, the positions of the Ru bands are mainly defined by the crystal field, which, in turn, is mainly due to Ru-O hybridization. The odd combination of Ru *d* orbitals does not hybridize with the bridging oxygen, and thus is less pushed up than the even one.
[45] M. Braden, W. Reichardt, S. Nishizaki, Y. Mori, and Y. Maeno, Phys. Rev. B **57**, 1236 (1998).
[46] I. Hase and Y. Nishihara, J. Phys. Soc. Jpn. **66**, 3517 (1997).
[47] D.J. Singh, *Planewaves, Pseudopotentials and the LAPW Method* (Kluwer Academic, Boston, 1994).
[48] D. Singh, Phys. Rev. B **43**, 6388 (1991).
[49] LAPW sphere radii of 2.1, 2.0, and $1.65a_0$ were used for Sr, Ru, and O, respectively. An LAPW sector basis set cutoff of $4.55a_0^{-1}$ was used with the addition of local orbitals for the Sr *s* and *p*, Ru *s*, *p*, and *d*, and O *s* channels.
[50] W.E. Pickett, H. Krakauer, and P.B. Allen, Phys. Rev. B **38**, 2721 (1988); D.G. Shankland, in *Computational Methods in Band Theory*, edited by P. Marcus, J. Janak, and A. Williams (Plenum, New York, 1971), p. 362.
[51] Program SURFER, by Golden Software; the Fourier method yielded smoother curves, while this minimum curvature approach yielded slightly better behavior near crossings and anticrossings.
[52] P. Aebi, J. Osterwalder, P. Schwaller, L. Schlapbach, M. Shimoda, T. Mochiku, and K. Kadowaki, Phys. Rev. Lett. **72**, 2757 (1994).
[53] D.J. Singh and W.E. Pickett, Phys. Rev. B **51**, 3128 (1995).
[54] H.M. Fretwell, A. Kaminski, J. Mesot, J.C. Campuzano, M.R. Norman, M. Randeria, T. Sato, R. Gatt, T. Takahashi, and K. Kadowaki, Phys. Rev. Lett. **84**, 4449 (2000).
[55] S.V. Borisenko, M.S. Golden, S. Legner, T. Pichler, C. Durr, M. Knupfer, J. Fink, G. Yang, S. Abell, and H. Berger, Phys. Rev. Lett. **84**, 4453 (2000).
[56] P.K. de Boer and R.A. de Groot, Phys. Rev. B **59**, 9894 (1999). In this work generalized gradient approximation calculations with a magnetization of $0.5\mu_B$/Ru are reported for Sr_2RuO_4. While that material is nonmagnetic both experimentally and in LSDA calculations, the magnetic interactions across the rock-salt layers should be of the same order as in $Sr_3Ru_2O_7$ based on the similar chemistry and structure.
[57] J.M. Kosterlitz and D.J. Thouless, J. Phys. C **6**, 1181 (1973).
[58] Y. Maeno, K. Yoshida, H. Hashimoto, S. Nishizaki, S.-I. Ikeda, M. Nohara, T. Fujita, A.P. Mackenzie, N.E. Hussey, J.G. Bednorz, and F. Lichtenberg, J. Phys. Soc. Jpn. **66**, 1405 (1997).